Building Tomorrow's Society

Bâtir la Société de Demain

Fredericton, Canada

June 13 – June 16, 2018/ *Juin 13 – Juin 16, 2018*

THE ROLE OF ROCK DIRECT SHEAR TESTING AND PRACTICAL ASPECTS OF BOUNDARY CONDITIONS

Packulak, Timothy R.[1,3] and Day, Jennifer J.[2]
[1] Dept. of Geological Sciences and Geological Engineering, Queen's University, Kingston, ON, Canada
[2] Dept. of Earth Sciences, University of New Brunswick, Fredericton, NB, Canada
[3] t.packulak@queensu.ca

Abstract: Laboratory constant normal load/stress (CNL/CNL*) boundary conditions in rock direct shear tests are achieved by maintaining the normal actuator at a constant load/stress, which allows the joint to dilate. Constant normal stiffness (CNS) boundary conditions differ as the machine is programed to maintain the normal stiffness, so as the joint dilates, the normal stress increases. While CNL* conditions are well documented and straightforward, a detailed literature review of CNS tests has revealed few details regarding appropriate laboratory testing protocols and data analysis. This paper presents practical guidelines needed to design an effective CNS test suite on pre-existing fracture samples that can be applied to a variety of rock types, based on intact rock elastic properties and recommended deformation properties from analysis of laboratory data. Deformation and yield properties of direct shear samples including normal stiffness, shear stiffness, shear strength, and post-yield dilation behaviour are analyzed in this study. In particular, new practical methods to determine dilation and total dilation potential are discussed. These properties are all needed to provide parameter inputs that accurately define the mechanical behaviour of rock joints in explicit and discrete geomechanical numerical models. Finally, discrete element method numerical models are used in this study to illustrate differences between numerical models of laboratory scale direct shear tests using input properties from the CNL* and CNS laboratory test conditions, with a focus on the effects of dilation angle and dilation potential.

1 INTRODUCTION

Laboratory direct shear testing is an essential tool that is used to characterize the stiffness, strength, and post-yield dilation behaviour of rock joints and other fractures in geotechnical engineering. Constant normal stress (CNL*) and constant normal load (CNL) boundary conditions represent fracture behaviour in slopes and other near surface gravity-driven environments. Constant normal stiffness (CNS) boundary conditions are better suited to simulate rock fractures near underground excavations, such as tunnels, mines, and nuclear waste repositories, where in situ and induced stresses dominate rockmass behaviour (Goodman 1976; Indraratna et al. 1999). While CNL and CNL* conditions allow the fracture to dilate freely during shear, so there is no feedback between dilation and normal stress, dilation is constrained by this feedback in CNS conditions. Determining appropriate geomechanical properties of fractures in granitic rock under CNL* and CNS boundary conditions is the focus of this investigation.

2 CONSTANT NORMAL STIFFNESS (CNS)

The CNS boundary condition constrains dilation during shearing. This causes the normal stress to increase, which in turn increases shear resistance (Indraratna et al. 1999). CNS conditions are intended to simulate conditions observed in underground environments, rock socketed piles, and bolted joints where dilation is constrained (Figure 1). In direct shear laboratory testing, a machine input for normal stiffness (KNM), rather than a constant stress used in CNL and CNL* tests, is applied to the specimen during the shear stage in order to replicate the confining environment associated with these real world situations. The CNS boundary

condition can be applied in the laboratory with servo-control or with springs (Figure 2). The increase in normal stress on the test specimen during shear is equal to KNM × d_n, where d_n is the normal displacement (dilation) of the discontinuity in millimeters.

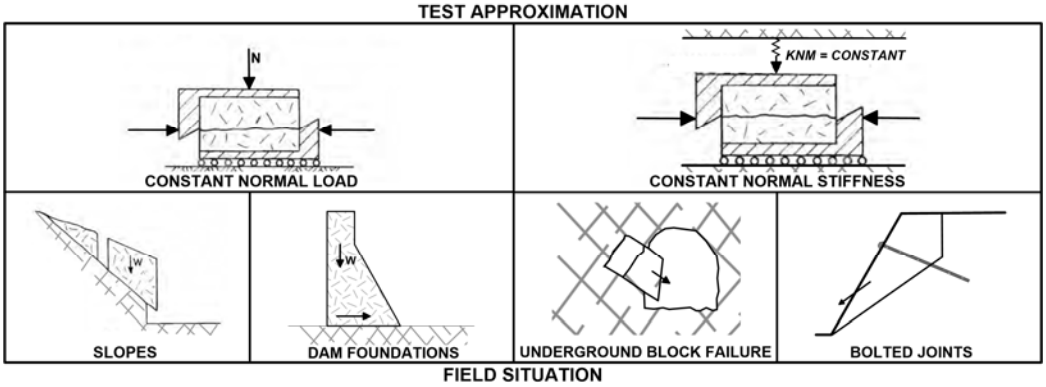

Figure 1: Examples of joint boundary conditions in situ and their lab equivalent. Modified after Goodman (1976) and Haverfield and Szymakowski (2003)

3 CREATING A DIRECT SHEAR TESTING PROGRAM

Prior to the development of servo-controlled direct shear machines, CNS boundary conditions were applied by springs with a known stiffness (Johnston et al. 1987) (Figure 2E). Springs limit the available machine normal stiffness (KNM) magnitudes under CNS to springs that can be produced and procured. Servo-controlled equipment allows for greater freedom in choosing KNM magnitudes that may be more representative of the underground environment of interest.

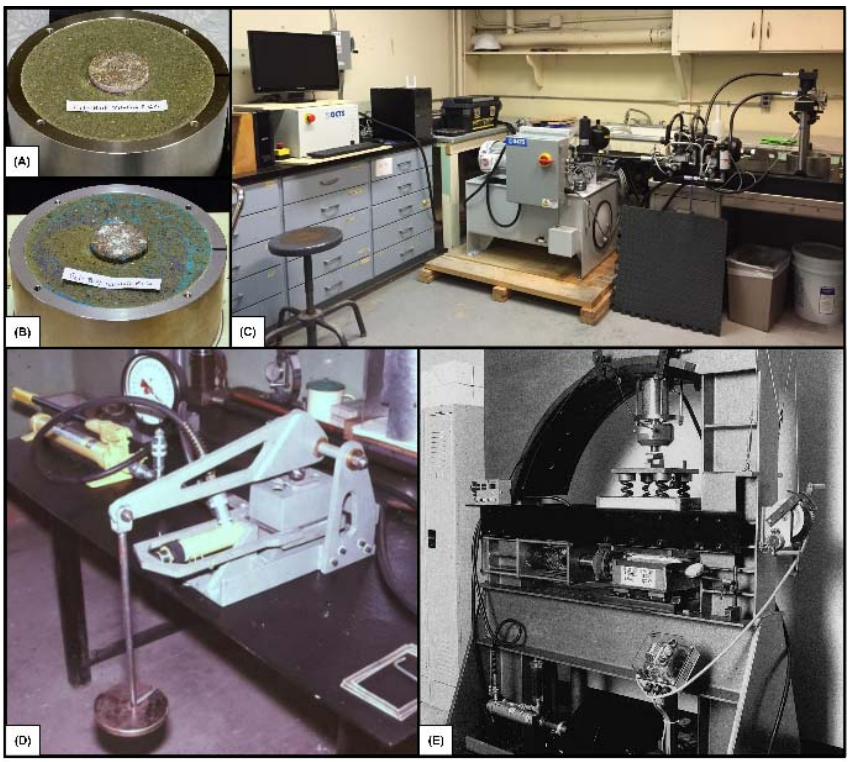

Figure 2: Testing Specimens and Equipment; (A) Granite specimen pre-shear, (B) Granite specimen post-shear, (C) Queen's University Advanced Geomechanics Testing Laboratory (AGTL) GCTS RDS 200 servo-controlled direct shear machine (CNL* and CNS), (D) Constant normal load direct shear machine, weights are applied to the arm to sustain a constant load and the hydraulic jack is used to apply a shear

force (Hoek 2007), (E) Constant normal stiffness direct shear machine, springs have been applied to a constant normal load machine to create the constant normal stiffness condition (Indraratna et al. 1999)

The applied machine stiffness can be estimated by the global normal stiffness of the system. The first developments of equations to estimate the global normal stiffness of a rockmass are based on the dilation and shear behaviour exhibited by a concrete pile near ground surface (Johnston et al. 1987). These equations do not fully capture the behaviour of planar rockmass fractures in underground environments. Work by Skinas et al. (1990) and Thirukumaran and Indraratna (2016) was helpful in the work to develop the following equation for machine normal stiffness (Packulak et al. 2018):

$$[1]\quad KNM = \frac{E}{2L \times (1-v^2)} \times A$$

where A is sample area, L is rockmass joint spacing, E is Young's Modulus, and v is Poisson's Ratio. Equation 1 is based on the consideration of a rockmass system of intact rock (defined by E and v), cut by infinitely repeating parallel joints with a spacing of L that simultaneously dilate under identical boundary conditions. The relationship in Equation 1 estimates KNM, which is the simulated stiffness of the machine for CNS tests performed with springs; this would be the spring constant.

Once KNM has been determined based on the sample geometry and material properties, and using Equation 1, an appropriate range of confining stresses for the test program is required. A laboratory test program should contain at least three different applied normal stress conditions. According to the International Society for Rock Mechanics suggested methods (Muralha et al. 2013), between three and five specimens should be tested at each boundary condition on fractures from the same joint or test horizon. This is ideally suited for oriented drill core; for unoriented core where it is difficult to identify joint sets, test specimens should have similar surface characteristics such as roughness, alteration and mineral coating. Further guidelines for sample selection are presented by Day et al. (2017).

4 PRE-YIELD DEFORMATION BEHAVIOUR: STIFFNESS

The normal stiffness of a joint (K_n) is measured during the normal loading phase of a direct shear test, when there is zero shear loading. Several closure laws exist to determine K_n with respect to increasing normal stress. The empirical hyperbolic fracture closure law proposed by Goodman (1974) is asymptotic toward maximum joint closure. Hungr and Coates (1978) determined that joints that have been exposed to higher stresses in situ than those applied in the lab exhibit a linear relationship between stress and displacement. Zangerl et al. (2008) implemented a semi-logarithmic closure law proposed by Bandis et al. (1983), together with the stiffness characteristic by Evans et al. (1992), to describe the non-linear behaviour of closure data. An extensive suite of normal stiffness results comparing the linear and semi-logarithmic closure laws is presented by Day et al. (2017). In order to estimate K_n, all test results from the normal loading stage (zero shear load) collected by the authors have thus far been analyzed using both linear (Hungr and Coates 1978) and semi-logarithmic (Zangerl et al. 2008) closure relationships.

To determine joint shear stiffness (K_s), the slope of the shear stress (tau) versus shear displacement (δ_s) curve is measured between the start of shearing and the peak shear strength. The determinations of secant (K_{SS}, zero to peak), tangent (K_{ST}, at 50% of peak shear strength), and chord (K_{SC}, linear-elastic portion of the tau versus δ_s) are based on guidelines by Day et al. (2017). Testing completed by the authors shows that joint shear stiffness (K_s) is dependent on the magnitude of applied normal stress, but K_s is not affected by different boundary conditions (CNL* versus CNS).

5 YIELD AND POST-YIELD BEHAVIOUR: SHEAR STRENGTH

Fractures tested under CNL* conditions show two distinct failure envelopes: "yield strength" (also the maximum strength) and "residual strength" (after some slip). Under CNS conditions, an initial "yield strength" is recorded (first slip), followed by a hardening behaviour (due to dilational feedback) up to a "maximum strength", and followed by a decrease to "residual strength" after additional shear displacement.

Prior to yield, there is no significant dilation and therefore the normal stress remains relatively constant. Post-yield, three behaviours with varying impacts on dilation are possible: sliding along asperities, shearing

through asperities or major crushing of asperities (Johnston and Lam 1989). All three behaviours result in an initial opening of the discontinuity and potential closing as shearing progresses, resulting in variations of normal stress under CNS conditions. As shearing continues, the joint will dilate due to sliding over the surfaces of asperities, causing an increase in normal stress, and in turn increasing the shear resistance. Once the shear stress of sliding along the asperity exceeds its shear strength, a new shear plane develops through the asperity. It is at this point the fracture shear strength drops to a residual state from maximum strength.

The shear strength results from laboratory tests completed in this research (Figure 3) are sorted by boundary condition (CNL*, and CNS – 6 kN/mm) and plotted with linear best-fit Mohr-Coulomb strength envelopes (Mohr-Coulomb properties are listed in Table 1). Residual shear strength data for tests with post-yield grout interference are not included in these best-fit calculations (Packulak et al. 2018A). As the samples used in this test program are medium and coarse grained, unfoliated to slightly foliated granites and gneisses, the scatter is associated with the variability in crystal strength, asperity height, and any potentially pre-existing structures. The point of maximum shear strength in CNS testing represents the point where asperity sliding is overcome by asperity shearing and the development of new shear planes as described in Johnston et al. (1987).

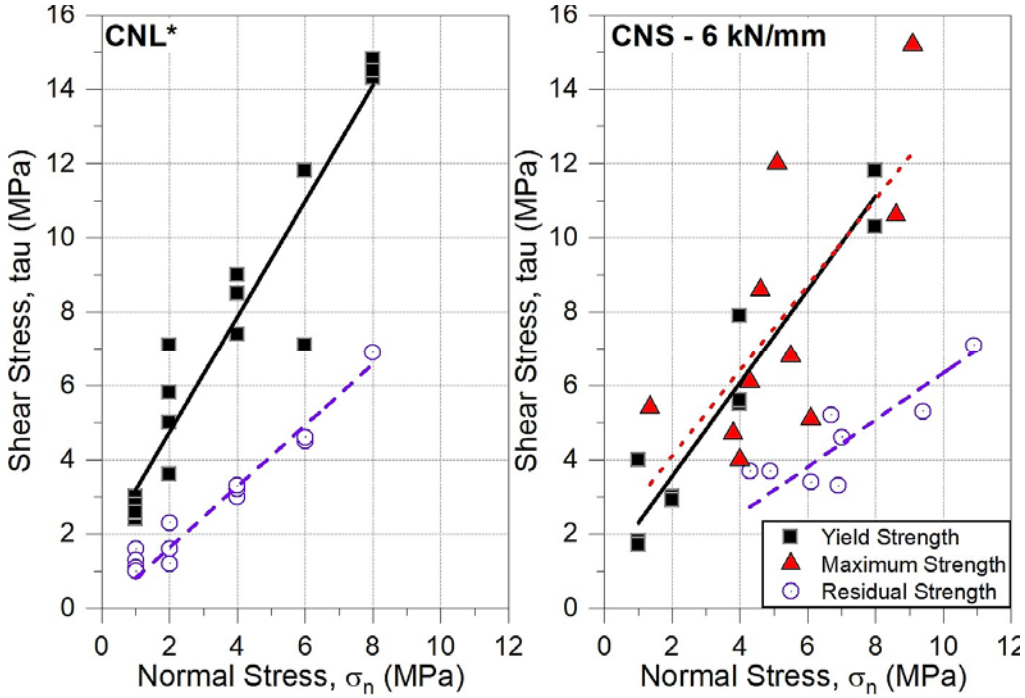

Figure 3: Mohr-Coulomb strength envelopes for CNL* (16 completed tests) and CNS-6 (12 completed tests), properties are in Table 1.

Table 1: Summary of Mohr-Coulomb shear strength parameters for all boundary conditions

Boundary Condition	Yield Shear Strength			Maximum Shear Strength			Residual Shear Strength		
	φ_y [°]	c [MPa]	R^2	φ_m [°]	c [MPa]	R^2	φ_r [°]	c [MPa]	R^2
CNL*	57.3 ± 7.7	1.6 ± 0.6	0.90	N/A	N/A	N/A	39.4 ± 1.8	0	0.98
CNS-6	51.6 ± 7.6	1.0 ± 0.6	0.91	49.1 ± 21.6	1.8 ± 2.2	0.51	32.4 ± 2.1	0	0.98

6 POST-YIELD BEHAVIOUR: DILATION

Dilation is an important characteristic that describes post-yield behaviour of rock fractures (Bandis et al. 1983). A new approach to determine a secant dilation angle (ψ_s) is proposed in this research to address input requirements for joint elements in discrete numerical models. An example measurement of ψ_s from

shear stress (tau) and normal displacement (δ_n) versus shear displacement (δ_s) data is shown in Figure 4. First, the shear strength yield point (A) and a zone of shear displacement (B to C) that is representative of residual shear strength are selected. ψ_s is the angle from horizontal that is formed from drawing a line from the yield point on the normal displacement curve (A) to the start of residual shear strength zone on the normal displacement curve (B) (Figure 4). The total dilation potential (δ_{nm}), for numerical modelling purposes, is the amount of dilation from yield (Figure 4, point A) to the end of what is determined to be the end of representative residual behaviour (Figure 4, point C).

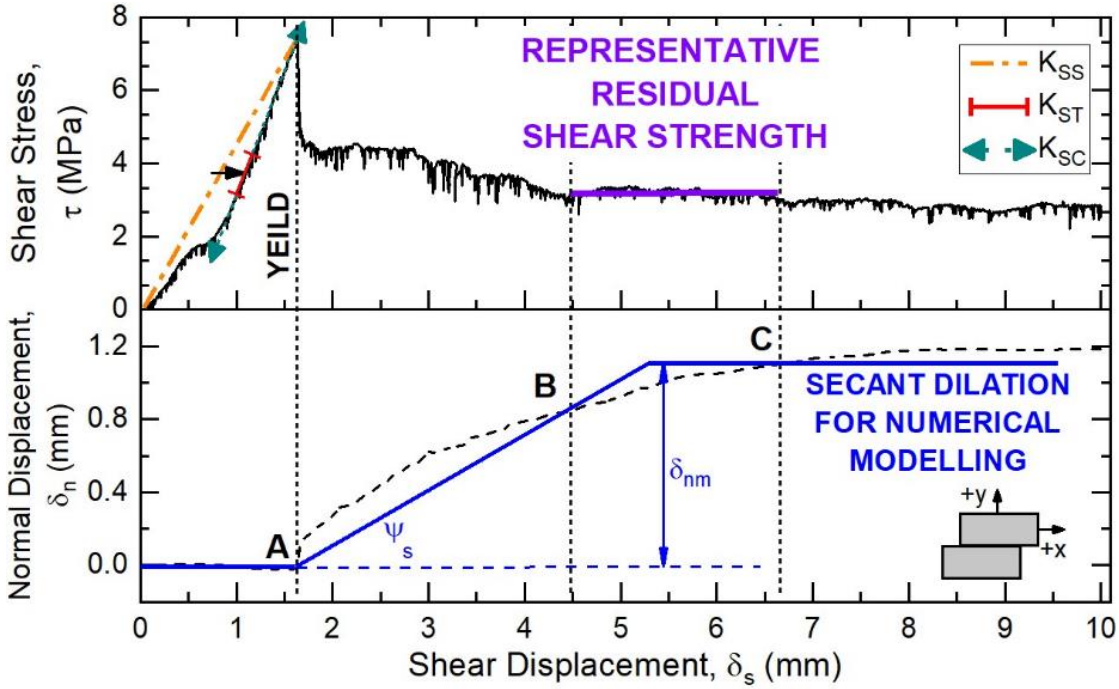

Figure 4: Example shear stress (tau) and normal displacement (δ_n) results (CNL*) (laboratory testing conducted by the authors) with new secant dilation angle (ψ_s) and total dilation potential (δ_{nm}) measurements

7 NUMERICAL MODELLING SOFTWARE MECHANICS

To analyze laboratory-scale shear behaviour, the Distinct Element Method (DEM) Universal Distinct Element Code (UDEC) by Itasca Consulting Group Inc. (2014) was used. In DEM codes, material domains are divided into discrete blocks with contacts between blocks that must be continuously identified and updated during every time step (Jing 2003). Updates to block contact forces and displacements are calculated at each time-step during the deformation process and are based on equations of motion, a defined geomechanical constitutive model and boundary conditions (Itasca 2014). In UDEC, there are multiple built-in geomechanical constitutive models for joint stiffness and strength, which were developed at different times during the evolution of rock mechanics. This study focused on the use of the Mohr-Coulomb (M-C) (Coulomb 1776) constitutive model and its associated consideration of joint dilation parameters.

8 MODEL SETUP

Three separate numerical models were created using UDEC (Itasca 2014) software. Details about the model setup and boundary condition are illustrated in Figure 5. Three separate laboratory scale test cases are presented: (A) CNL flat joint, (B) CNL triangular joint, and (C) CNS flat joint. The rock material selected for this study is granite. Results from unconfined compressive strength tests as presented in Packulak et al. (2018B) are summarized as follows: a unit weight of 0.026 MN/m^3, an intact Young's Modulus of 75,536 MPa and a Poisson's ratio of 0.29 (with a corresponding bulk modulus of 58,555 MPa and shear modulus of 29,391 MPa). The CNS direct shear boundary condition model shown in Figure 5C is used to simulate the boundary condition. The spring block is assigned material properties such that external constant normal

machine stiffness (6 kN/mm and 12 kN/mm) is modelled explicitly. In order to prevent unconfined dilation from occurring in the system, the top of the spring block is pinned in place after the initial stress has been applied, after the model has reached equilibrium, and prior to shearing. The CNL direct shear test is modelled in a similar way as the CNS condition, except that the spring block has been removed and the top boundary of the top specimen block is left free. In order to determine the physical properties of the "spring" block in UDEC, a Young's Modulus was determined using Eq. 1, and then used to calculate Bulk and Shear Moduli (Table 2).

Table 2: Material properties for the spring block used in UDEC CNS flat joint model C

Machine Normal Stiffness [kN/mm]	Young's Modulus [MPa]	Bulk Modulus [MPa]	Shear Modulus [MPa]
6	158	53	79
12	317	106	158

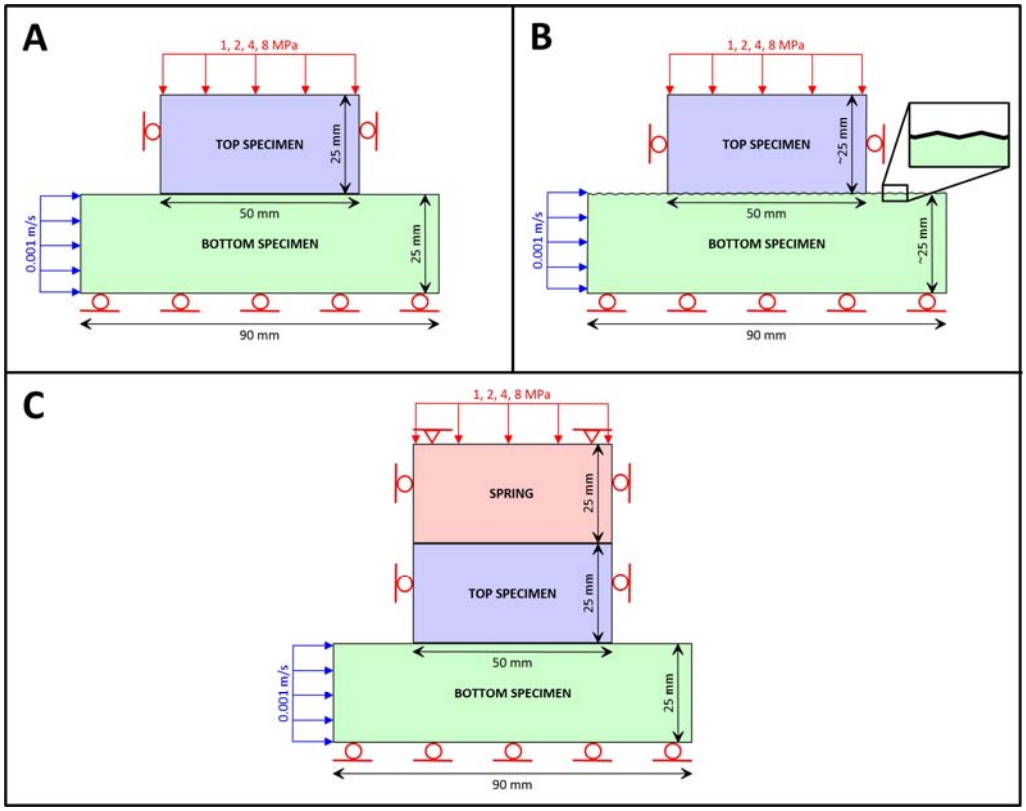

Figure 5: Diagrams of the direct shear test models in UDEC, including the model geometry, external boundary conditions, normal loading conditions, and applied velocity; (A) CNL setup with flat joint, (B) CNL setup with triangular joint, where asperity height and angle of asperity was varied, and (C) CNS setup with flat joint

9 NUMERICAL MODELLING RESULTS & DISCUSSION

Using the M-C constitutive model, dilation can be modelled through the "jdilation" parameter or through physical asperities. The normal displacement versus shear displacement results for CNL models (Figure 6A) and CNS models (Figure 7) show the dilatational behaviour for flat jointed models using the "jdilation" parameter. Dilation behaviour for flat jointed models is compared to physically modeled asperities in Figure 6B. As shown in Figure 6A, the joint remains closed until the model begins to dilate, which is determined based on applied normal stress. Prior to shearing, the normal stress is applied and the model is allowed to go to equilibrium, as the models have the same strength and stiffness characteristics failure / dilation occurs later in the shearing phase. In Figure 6B, due to model parameters, the bottom block is deforming and being compressed as shearing progresses. This deformation has produced an overall negative total

displacement as shown in Figure 6B. This phenomenon can be improved with adjusting model parameters and placing history points above and below the fracture to determine the dilative component instead of total deformation of the model. Figure 6B does not fully represent dilation occurring in the model. Numerical results from CNS models show a dampening of the dilation angle under the 12 kN/mm stiffness from 20° to just over 10° (Figure 7). For other boundary conditions there does not appear to be a dampening of the dilation angle.

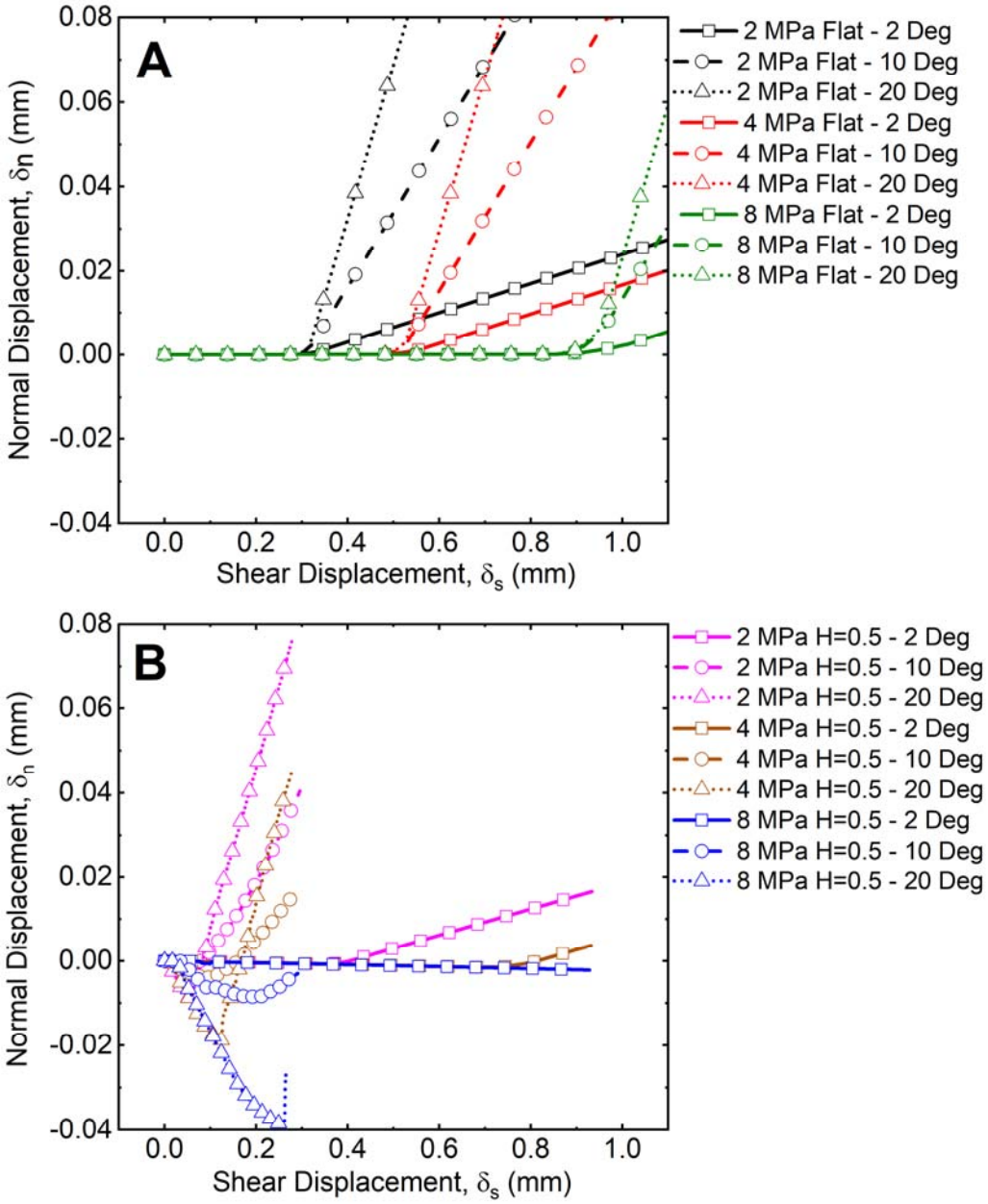

Figure 6: Normal displacement versus shear displacement graphs showing dilation characteristics for joints with dilation angles of 2°, 10°, and 20° with respect to stress. (A) CNL setup with flat joint (Figure 5A); (B) CNL setup with triangular joint (Figure 5B) asperity height of 0.5 mm

Smaller shear displacement values needed before the joint starts to dilate (Figures 6 and 7) directly influences when yield occurs in terms of shear stress versus shear displacement (Figure 8). In Figure 8A, CNL models with flat joints are not directly impacted by dilation as controlled in the model by the “jdilation” parameter, which is not the case in reality. CNL tests with explicitly modelled asperities show a dependence on dilation angle and asperity height with respect to yield shear strength. Joints with lower dilation angles

show a smaller drop from yield shear strength to residual strength under CNL conditions. Flat jointed CNS model results show yield occurring earlier during the shearing stage and at lower shear strengths when compared to flat jointed CNL models (Figure 8B). The CNS model has the linear elastic pre-yield section, which occurs before significant dilation takes place, at the point in the model where dilation starts to occur the model immediately drops to a residual state. In laboratory results, an increase in normal stress increases the shear resistance leading to a "maximum strength", which does not appear in the numerical results. The CNS condition has an effect in the post-yield region where shear resistance increases as shearing continues.

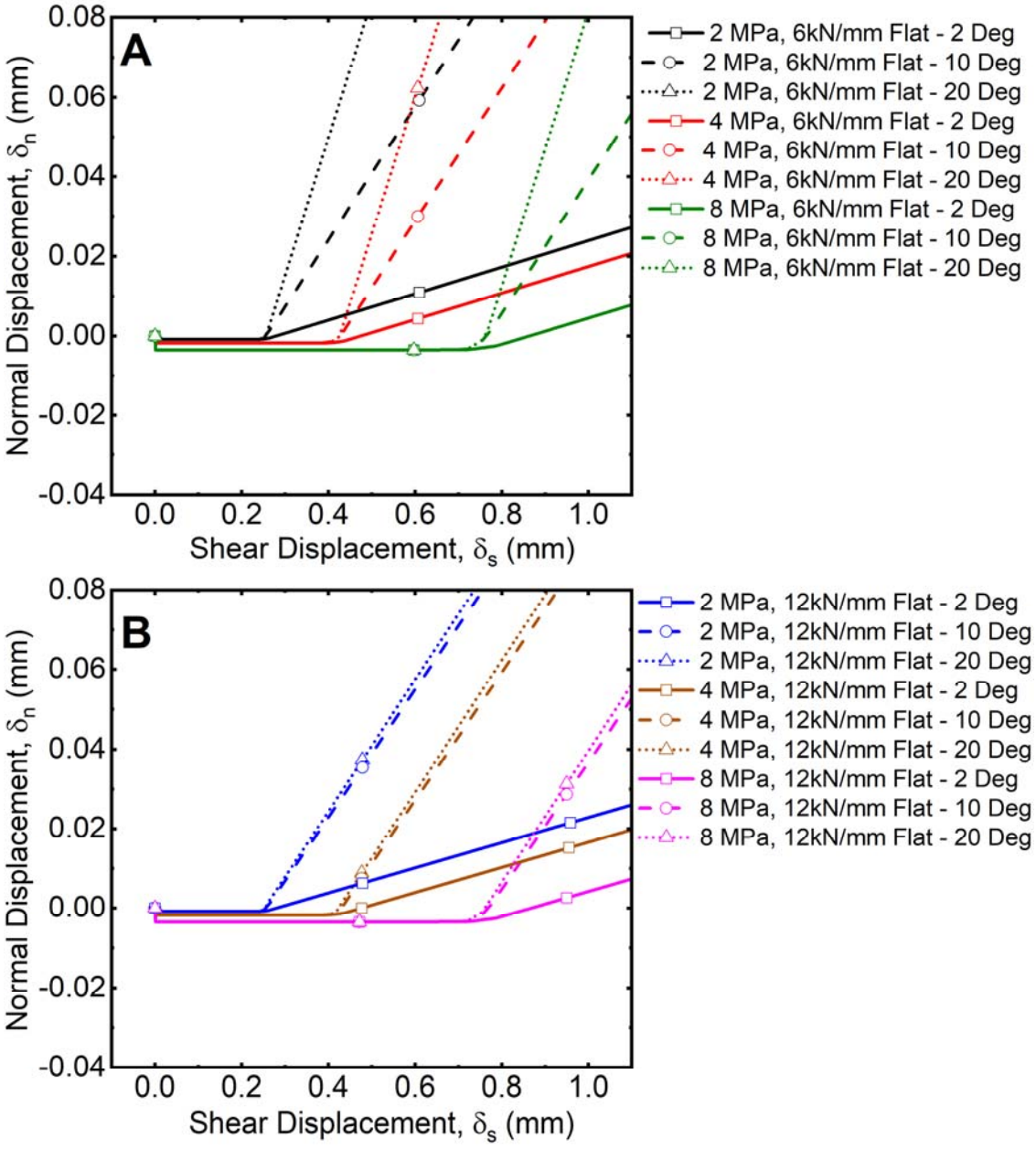

Figure 7: Normal displacement versus shear displacement graphs showing dilation characteristics for joints with dilation angles of 2°, 10°, and 20° with respects to stress. (A) CNS setup with flat joint (Figure 5C) and a system stiffness (KNM) of 6 kN/mm (B) CNS setup with flat joint (Figure 5C) and a system stiffness (KNM) of 12 kN/mm

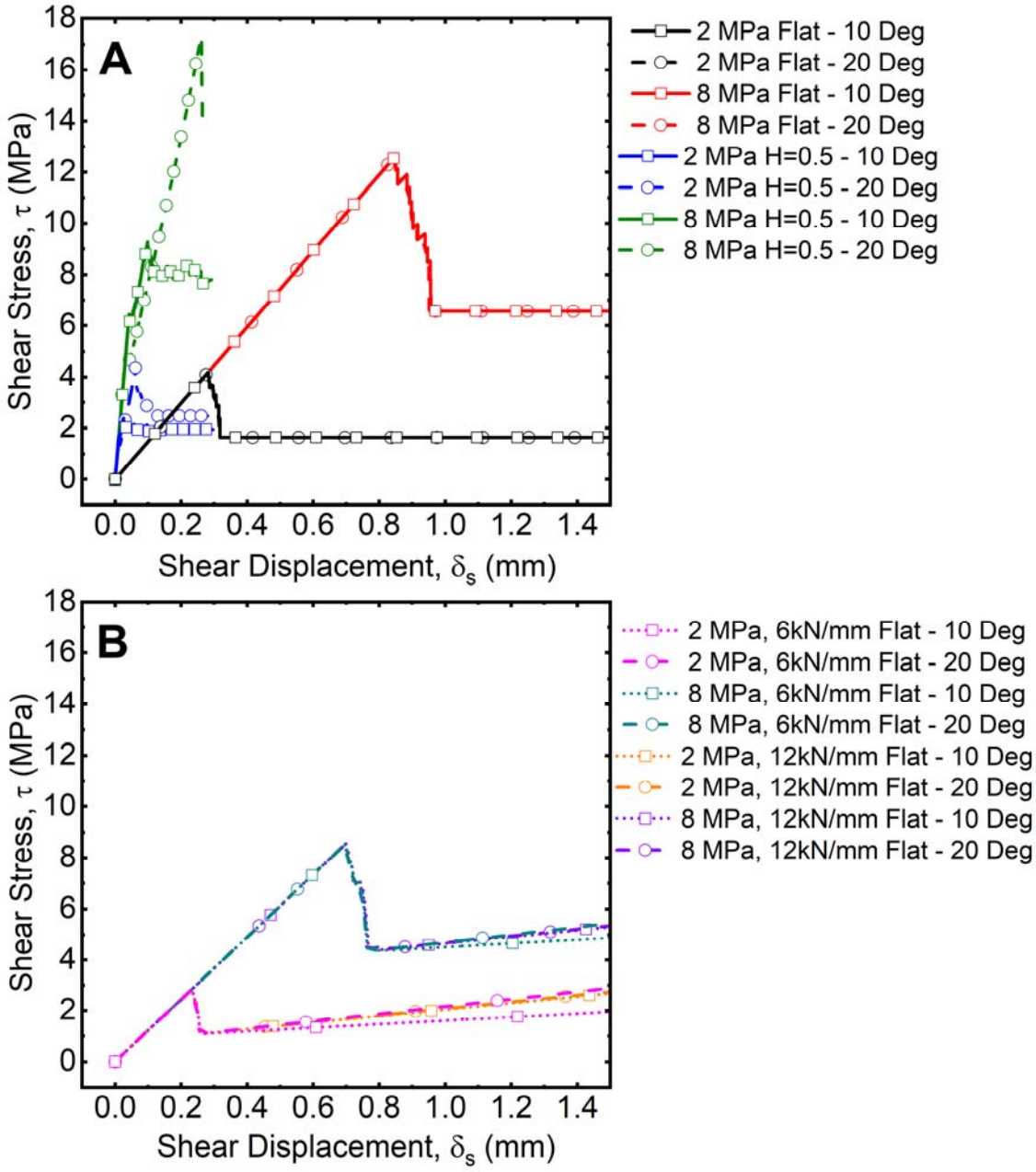

Figure 8: Graphs showing shear stress versus shear displacement profiles from models with applied normal stresses of 2 MPa and 8 MPa with dilation angles of 10° and 20°; (A) CNL boundary conditions for flat and triangular joints, (B) Flat joint CNS boundary condition with machine normal stiffness values of 6 kN/mm and 12 kN/mm

10 CONCLUSIONS

The new equation for machine normal stiffness (KNM) provides a means to target appropriate CNS boundary conditions in direct shear testing for rockmass properties of interest, which better reflects rockmass behaviour around an underground excavation. The proposed secant dilation angle (ψ_s) provides an improved approach to measuring dilation for numerical modelling applications. Pre-yield parameters such as joint normal stiffness and shear stiffness have thus far been observed to be independent of the test boundary condition, as the CNS component does not take full effect until peak shear strength has been reached. For the numerical modelling of direct shear problems, using the M-C constitutive model is not

appropriate for flat jointed CNS conditions as the influence of the CNS condition occurs after the model has started using the residual parameters. To improve the shear behaviour of joints in numerical models, future work will investigate alternative constitutive models that capture the transition observed in laboratory test data from peak to residual shear behaviour.

ACKNOWLEDGMENTS

The Natural Sciences and Engineering Research Council of Canada, the Nuclear Waste Management Organization of Canada and the Tunnelling Association of Canada have financially supported this research. Manitoba Hydro and KGS Group Consulting Engineers supplied the rock core samples.

REFERENCES

Bandis, S.C., Lumsden, A.C. and Barton, N.R. 1983. Fundmentals of Rock Joint Deformation. *International Journal of Rock Mechanics, Mining Sciences and Geomechanics Abstracts,* **20**(6): 249-268.

Coulomb, C.A. 1776. Essa sur une application des regles des maximis et minimis a quelquels problemesde statique relatifs, a la architecture. *Mem. Acad. Roy. Div. Sav.* 7: 343-387.

Day, J.J., Diederichs, M.S. and Hutchinson, D.J. 2017. New direct shear testing protocols and analyses for fractures and healed intrablock rockmass discontinuities. *Engineering Geology*, **229**: 53-72.

Evans, K.F., Kohl, T., Rybach, L. and Hopkirk, R.J. 1992. The effects of fracture normal compliance on the long term circulation behaviour of a hot dry rock reservoir: a parameter study using the new fully-coupled code "FRACTure". *Geothermal Resources Council Transactions*, **16**: 449-456.

Goodman, R.E. 1976. *Methods of Geological Engineering in Discontinuous Rocks.* West St. Paul: West Publishing Company.

Goodman, R.E. 1974. "The mechanical properties of joints." *3rd International Congress of the International Society of Rock Mechanics.* 1-7.

Haberfield, C.M. and Szymakowski, J. 2003. Applications of Large Scale Direct Shear Testing. *Australian Geomechanics*, 29-39.

Hoek, E. 2007. *Practical Rock Engineering.* Toronto.

Hungr, O. and Coates, D.F. 1978. Deformability of joints and its relation to rock foundation settlements. *Canadian Geotechnical Journal*, **15**(2): 239-249.

Indraratna, B., Haque, A. and Aziz, N. 1999. Shear behaviour of idealized infilled joints under constant normal stiffness. *Geotechnique*, **49**(3): 331-355.

Itasca Consulting Group Inc. 2014. UDEC: Universal Distinct Element Code v. 6.0. www.itascacg.com. Minneapolis, MN.

Jing, L. 2003. A review of techniques, advances, and outstanding issues in numerical modelling for rock mechanics and rock engineering. *International Journal of Rock Mechanics and Mining Sciences*, **40**: 283-353.

Johnston, I.W. and Lam, T.S. 1989. Shear behaviour of regular triangular concrete/rock joints - analysis. *Journal of geotechnical engineering*, **115**(5): 711-727.

Johnston, I.W., Lam, T.S.K. and Williams, A.F. 1987. Constant Normal Stiffness Direct Shear Testing for Socketed Pile Design in Weak Rock. *Geotechnique* **37**(1): 83-89.

Muralha, J., Grasselli, G., Tatone, B., Blumel, M., Chryssanthakis, P. and Yujing, J. 2013. ISRM Suggested Method for Laboratory Determination of the Shear Strength of Rock Joints: Revised Version. *Rock Mechanics and Rock Engineering*, **47**: 291-302.

Packulak, T.R., Day, J.J. and Diederichs, M.S. 2018A. Assess: The role of rock direct shear testing in determining geomechanical properties of fractures. *Tunnels and Tunnelling*, Feb-Mar: 32-36

Packulak, T.R., Day, J.J. and Diederichs, M.S. 2018B. Practical aspects of boundary condition selection on direct shear laboratory tests. *2018 European Rock Mechanics Symposium*. St. Petersburg: CRC Press.

Skinas, C.A., Bandis, S.C. and Demiris, C.A. 1990. Experimental investigations and modelling of rock joint behaviour under constant stiffness. Eds. N. Barton and O. Stephansson. *The International Symposium on Rock Joints.* Rotterdam, A.A.Balkema: 301-308.

Thirukumaran, S. and Indraratna, B. 2016. A review of shear strength models for rock joints subjected to contant normal stiffness. *Rock Mechanics and Geotechnical Engineering*, **8**(3): 405-414.

Zangerl, C.,Evans, K.F., Eberhardt, E. and Loew, S. 2008. Normal Stiffness of fractures in granitic rock: A compilation of laboratory and in-situ experiments. *Int. J. Rock Mech. & Min. Sci.*, **45**(8): 1500-1507.